CHEMISTRY
A European Journal

A Journal of
ChemPubSoc Europe

Accepted Article

Title: Cooperative and Independent Effect of Modular Functionalization on Mesomorphic Performances and Microphase Separation of Well-Designed Liquid Crystalline Diblock Copolymers

Authors: Lan Lei, Li Han, Hongwei Ma, Ruixue Zhang, Shuai Huang, Heyu Shen, Lincan Yang, Chao Li, Songbo Zhang, Hongyuan Bai, Qingchi Ma, and Yang Li

To be cited as: *Chem. Eur. J.* 10.1002/chem.202000268

Link to VoR: http://dx.doi.org/10.1002/chem.202000268

Supported by
ACES

WILEY-VCH

10.1002/chem.202000268

WILEY-VCH

Cooperative and Independent Effect of Modular Functionalization on Mesomorphic Performances and Microphase Separation of Well-Designed Liquid Crystalline Diblock Copolymers

Lan Lei, Li Han,* Hongwei Ma, Ruixue Zhang, Shuai Huang, Heyu Shen, Lincan Yang, Chao Li, Songbo Zhang, Hongyuan Bai, Qingchi Ma, and Yang Li*

L. Lei, Dr. L. Han, Prof. H. W. Ma, R. X. Zhang, S. Huang, H. Y. Shen, L. C. Yang, C. Li, S. B. Zhang, H. Y. Bai, Q. C. Ma, and Prof. Y. Li
State Key Laboratory of Fine Chemicals, Department of Polymer Science and Engineering, Liaoning key Laboratory of Polymer Science and Engineering, School of Chemical Engineering, Dalian University of Technology, Dalian Liaoning 116024, China.
E-mail: liyang@dlut.edu.cn (Y. Li), hanli.dlut.edu.cn (L. Han)

Supporting information for this article is given via a link at the end of the document.

Abstract: Liquid crystalline block copolymers (LCBCPs) are promising for developing functional materials owing to assembly of better functionality. Taking advantage of difference in reactivity between alkynyl and vinyl over temperature during hydrosilylation, a series of LCBCPs with modular functionalization of block copolymers (BCPs) are reported by independently and site-selectively attaching azobenzene moieties containing alkynyl (LC_1) and Si-H (LC_2) terminals into well-designed poly(styrene)-block-polybutadienes (PS-*b*-PBs) and poly(4-vinylphenyldimethylsilane)-block-polybutadienes (PVPDMS-*b*-PBs) produced from living anionic polymerization (LAP). By the principle of modular functionalization, it is demonstrated that mono-functionalized (PVPDMS-*g*-LC_1)-*b*-PB and PS-*b*-(PB-*g*-LC_2) not only maintain independence but also have cooperative contributions to bi-functionalized (PVPDMS-*g*-LC_1)-*b*-(PB-*g*-LC_2) in terms of mesomorphic performances and microphase separation, which is evident from differential scanning calorimetry (DSC) and polarized optical morphologies (POM) and identified by powder X-ray diffractions. With the application of new principle of modular functionalization, local-crosslinked liquid crystalline networks (LCNs) with controlled functionality are successfully synthesized, which show well-controlled phase behaviors over molecular compositions.

Introduction

The principle of building "blocks" to assemble better functionality into a single molecular is becoming attractive towards driving specific functions.[1] To facilitate higher performance and gain innovative functionality, liquid crystalline block copolymers (LCBCPs) have received an unprecedented insight in molecular engineering and multifunctional materials.[2] As liquid crystalline (LC) and block copolymers (BCPs) with multiscale spatial orders are representative of self-organized systems, LCBCPs have an unpredictably cooperative and competitive motion between LC and BCPs order with control of compositions.[3] Furthermore, LCBCPs are generally composed of LC blocks and non-LC blocks served as rigid and flexible segments, which will induce spontaneous microphase separation due to thermodynamic differences of different blocks.[3b, 3e] For this reason, it is necessary that LCBCPs with well-controlled structures are developed to manipulate LC properties and microphase separation by tuning the motions between LC and BCPs order, as well as the thermodynamic differences of different blocks.

More and more researches of LCBCPs have been focused on the development of new synthetic methodologies, the discovery of new self-assembled morphologies, and the explorations of their applications in different fields.[2d, 3c, 4] A variety of synthetic methodologies have been developed to fabricate LCBCPs, for example, macromolecular induced conventional free radical polymerization of mesogenic moieties containing double bonds, and post-modification of BCPs containing OH/Cl side groups with mesogenic moieties, but they are lack of well-controlled structures.[5] As is known, the well-designed molecular weight and a narrow polydispersity index (PDI) are indispensable to achieve a basic molecular control. In recent years, many researches have applied macromolecular induced reversible addition-fragmentation chain-transfer polymerization (RAFT) to obtain the LCBCPs with well-controlled structures.[6] Therefore, the self-assembled morphologies of microphase separation have been well-controlled by varying chain length of BCPs and grafting density of LCBCPs.[3b, 7] However, few attempts have been made to reveal the independent and cooperative effect of different functions on LC properties and microphase separation of LCBCPs.[6a, 7b] The synthesis and complete characterization of LCBCPs with well-designed functions in different blocks of BCPs, i.e., modular functionalization, are challenging but valuable to be explored.[4a, 7a]

From the perspective of molecular manipulation, living anionic polymerization (LAP) is one of the best methods to obtain BCPs with well-controlled molecular weight and narrow PDI.[8] With regard to this field, our group has synthesized bi-functionalized BCPs templates,[9] and LCBCPs with a well-controlled grafting density in different blocks have been developed via highly efficient post-functionalization of mesogenic moieties with BCPs produced by LAP.[8a] However, a limitation remains regarding a site-selective functionalization of BCPs. To reveal an interior relationship between different functions, developing newly designed LCBCPs with modular functionalization, in which the specific functions are site-selectively incorporated into different blocks, is highly important.

As is known, funtionalization based on general polymers has become important to realize the synthesis of functioal materials with high performance. For this reason, poly(styrene-block-butadiene) (PS-*b*-PB) as a general polymer rubber has been taken into consideration to the synthesis of LCBCPs, because PS-*b*-PB rubbers that improve the mechanical performance and transparency depending on compositions have been widely used as thermoplastic elastomers.[10] However, unfunctionalized PSs have difficulties in achieving a post-functionalization and a site-selective manipulation in different blocks, which require a rational molecular design.

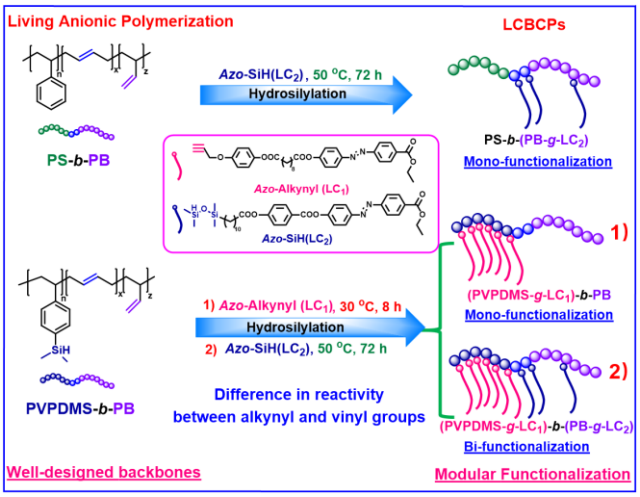

Scheme 1. Synthetic strategy of LCBCPs with modular functionalization.

In present work, much attention has been paid to poly(4-vinylphenyldimethylsilane)-block-polybutadiene (PVPDMS-*b*-PB) with Si-H in PVPDMS blocks and double bonds in PB blocks as bi-functionalized sites, because polybutadiene (PB) and poly(4-vinylphenyldimethylsilane) (PVPDMS) showed a high tunability of additional functionality in previous studies.[11] Taking advantage of difference in reactivity between alkynyl and vinyl groups over temperature during hydrosilylation, *Azo*-alkynyl (LC_1) and *Azo*-SiH (LC_2) with alkynyl and Si-H terminals are independently and site-selectively attached into PVPDMS-*b*-PBs and PS-*b*-PBs with well-designed degree of polymerization (DP) produced from LAP. As shown in Scheme 1, it is desirable to obtain LCBCPs with modular functionalization using a principle of "building" blocks, where the functional positions of grafted blocks and grafting density are controlled. The independent and cooperative effect of different functions is confirmed by mixing PB-*g*-LC_2 and PVPDMS-*g*-LC_1 in different mole ratios in comparison with LCBCPs, which is evident from DSC and POM results and identified on the basis of powder X-ray diffractions. We are inspired to apply this new principle to obtain the local-crosslinked liquid crystalline networks (LCNs) with reasonably designed functionality (Figure 4), as researchers have devoted much effort to the innovation of LCNs owing to the reversible order-disorder phase transition,[12] which will contribute to understanding the structure-property relations and further designing materials.

Results and Discussion

Synthesis of monomers and polymeric matrixes. Synthetic details and characterization for PVPDMS-*b*-PBs and PS-*b*-PBs with well-designed DP are according to previous report,[8a, 11c] which are briefly described in Supporting Information. Since *Azo* mesogens have been frequently incorporated into LCBCPs, alkynyl and Si-H terminated *Azo*-alkynyl (LC_1) and *Azo*-SiH (LC_2) have been synthesized and characterized as shown in Supporting Information. The characteristic peaks and their integrations in ^{1}H NMR of PVPDMS-*b*-PBs and PS-*b*-PBs are in good agreement with the designed structures, which are displayed in Figure S4-S5. GPC curves show a narrow and symmetric monomodal distribution (PDI=1.05-1.09) in Figure 1. As summarized in Table 1, PVPDMS-*b*-PBs and PS-*b*-PBs have well-controlled number-average molecular weight (M_n) and narrow PDI in different blocks. The self-crosslinking reaction of PVPDMS-*b*-PB occurred due to the hydrosilylation between Si-H of PVPDMS and double bonds of local PB blocks at 60 °C in previous work,[11c] and thus this work introduced alkynyl terminals in pursuit of LCBCPs with modular functionalization. Because alkynyl groups have a higher reactivity than double bonds at room temperature, which is desirable to obtain a selective addition in different blocks.[9c]

Synthesis of mono-functionalized LCBCPs. In this work, PVPDMS-*b*-PBs with different DP (Table 1) were firstly used for post-modification with alkynyl-terminated *Azo*-Alkynyl (LC_1). After performing the hydrosilylation of PVPDMS-*b*-PBs with *Azo*-Alkynyl (LC_1) at 30 °C, the synthetic process was tracked by ^{1}H NMR and FT-IR. As shown in Figure 1c, the appearance of δ (ppm) = 5.88 assigned to -Si(CH_3)$_2$-CH=C***H***- of LCBCPs and the disappearance of peaks δ (ppm) = 4.45 assigned to Si-***H*** of PVPDMS blocks in ^{1}H NMR indicated a complete addition of PVPDMS blocks with *Azo*-Alkynyl (LC_1). As shown in Figure S7, the complete addition was further determined by FT-IR with the disappearance of the absorption at 2116 cm^{-1} of Si-H groups in PVPDMS blocks. Moreover, the typical signals δ (ppm)= 5.68-4.85 of double bonds from PB blocks displayed no integral changes in ^{1}H NMR, which indicated that Si-H groups preferred to react with alkynyl groups of *Azo*-Alkynyl (LC_1) rather than double bonds of PB blocks in PVPDMS-*b*-PBs around room temperature when excessive *Azo*-Alkynyl (LC_1) was used. Therefore, a series of (PVPDMS-*g*-LC_1)-*b*-PB showed a block selective ability of mono-functionalization in PVPDMS blocks and an almost 100% grafting density. To achieve the mono-functionalizatin in PB blocks relative to PS blocks, PS-*b*-(PB-*g*-LC_2) as a contrast was synthesized after the treatment of *Azo*-SiH (LC_2) with PS-*b*-PB via hydrosilylation at 50 °C, which was supported by ^{1}H NMR (Figure 1d and S6a) and FT-IR (Figure S7) and described in Supporting Information.

Table 1. Molecular compositions and thermal properties of the designed BCPs.

Designed BCPs [a]	BCPs [b]		PS/PVPDMS[c]		PB [d]		Thermal Properties	
	M_n (kg/mol) [b]	PDI [b]	M_n (kg/mol) [c]	PDI [c]	M_n (kg/mol) [d]	1,4-PB(%) [e]	T_{g1} (°C) [f]	T_{g2} (°C) [f]
PS_{3k}-*b*-PB_{6k}	11.6	1.06	3.0	1.15	8.6	90.9	-93	17
PS_{3k}-*b*-PB_{12k}	15.4	1.05	3.2	1.13	12.2	91.7	-92	19
PS_{3k}-*b*-PB_{18k}	22.8	1.05	3.0	1.12	19.8	92.1	-94	21
$PVPDMS_{3k}$-*b*-PB_{6k}	10.4	1.06	4.2	1.13	6.2	90.1	-86	32
$PVPDMS_{3k}$-*b*-PB_{18k}	20.3	1.07	3.2	1.28	17.1	90.9	-91	29
$PVPDMS_{3k}$-*b*-PB_{30k}	33.7	1.09	4.0	1.15	29.7	91.6	-94	29

[a] BCPs with well-designed M_n (PS/PVPDMS) and M_n (PB) in different blocks. [b,c,d] Number-average molecular weight (M_n) and polydispersity index (PDI), determined by GPC. [c] PS and PVPDMS blocks of PS-*b*-PBs and PVPDMS-*b*-PBs, obtained by sampling. [d] PB blocks, determined by formula: M_n (PB)=M_n (BCPs)-M_n (PS/PVPDMS). [e] 1,4-PB mole fraction (%), calculated by ^{1}H NMR (shown in Figure S5). [f] The first glass transition temperature (T_{g1}) of PVPDMS and PS blocks, and the second glass transition temperature (T_{g2}) of PB blocks, determined by DSC.

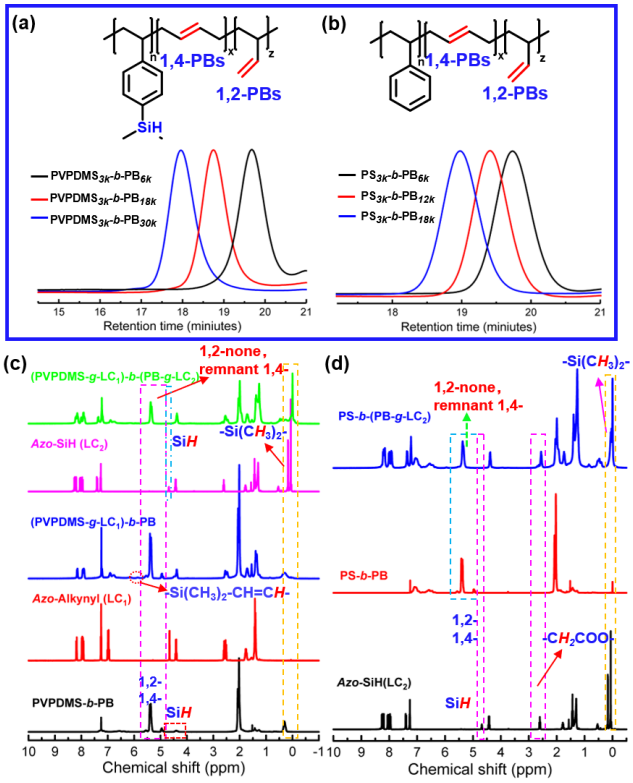

Figure 1. The GPC traces of (a) PVPDMS-*b*-PBs and (b) PS-*b*-PBs; ^{1}H NMR comparisons in the synthetic process of mono/bi-functionalized LCBCPs with *Azo* moieties (LC_1 and LC_2) and BCPs (PVPDMS-*b*-PBs and PS-*b*-PBs).

Synthesis of bi-functionalized LCBCPs. After performing the hydrosilylation of (PVPDMS-*g*-LC_1)-*b*-PB with *Azo*-SiH (LC_2) at 50 °C, the synthetic process was also detected by ^{1}H NMR. As shown in Figure 1c, the appearance of the peaks δ (ppm)= 0.16-0 of -Si-(C***H***$_3$)$_2$- from *Azo*-SiH (LC_2) and the disappearance of δ (ppm)=5.08-4.85 assigned to 1,2-PBs indicated the addition between *Azo*-SiH (LC_2) and 1,2-olefins of PB blocks. In addition, the remnant of the peaks δ (ppm)=5.68-5.23 assigned to 1,4-PBs was indicative of an incomplete addition in PB blocks. The grafting density in PB blocks was calculated according to Figure S8 and summarized in Supporting Information. Results strongly indicated that a series of bi-functionalized (PVPDMS-*g*-LC_1)-*b*-(PB-*g*-LC_2) were synthesized and showed a complete addition in PVPDMS blocks while an approximate 20% grafting density in PB blocks.

Fundamentally, the independent and cooperative effect of different functions in different blocks on mesomorphic performances and microphase separation can thus be investigated in terms of LCBCPs with modular functionalization, including mono-functionalized (PVPDMS-*g*-LC_1)-*b*-PB and PS-*b*-(PB-*g*-LC_2), and bi-functionalized (PVPDMS-*g*-LC_1)-*b*-(PB-*g*-LC_2) with different DP.

Polarized optical morphologies (POM). On the basis of POM observations in Figure 2a, the broken focal conical and spherical textures of *Azo*-Alkynyl (LC_1) as well as the focal conical and rod-like textures of *Azo*-SiH (LC_2) formed when heated and cooled. POM morphological variations of *Azo*-Alkynyl (LC_1) and *Azo*-SiH (LC_2) were indicative of the presence of LC phases and possible phase transitions. When *Azo*-Alkynyl (LC_1) and *Azo*-SiH (LC_2) were attached into PVPDMS-*b*-PBs and PS-*b*-PBs, the mesomorphic behaviors of mono/bi-functionalized LCBCPs were investigated. As shown in Figure 2b, LC morphological textures were observed in both mono/bi-functionalized LCBCPs. As in previous work, the textures of polymers were not well-formed due to highly flexible PB blocks.[8a] When adding pressure on the polarized film, the colorful morphologies formed drawing near to T_i. The morphological textures were observed in a brighter order: PS-*b*-(PB-*g*-LC_2)<(PVPDMS-*g*-LC_1)-*b*-PB<(PVPDMS-*g*-LC_1)-*b*-(PB-*g*-LC_2), which suggested that PB LC blocks and PVPDMS LC blocks of LCBCPs had cooperative contributions to the brighter textures of bi-functionalization.

Thermal Properties. As indicated in Figure 2a, DSC traces presented determinations of phase transitions of *Azo*-Alkynyl (LC_1) and *Azo*-SiH (LC_2). Except the melting temperature (T_m) and LC-isotropic temperature (T_i), the transition temperature of mesogenic phase (T_s) appeared in both *Azo*-Alkynyl (LC_1) and *Azo*-SiH (LC_2). Results indicated that *Azo*-SiH (LC_2) (T_i=187 °C, ΔT=116 °C) showed a much wider mesogenic temperature range (ΔT) value than did *Azo*-Alkynyl (LC_1) (T_i=90 °C, ΔT=32 °C) because of different terminal groups.

As is known, BCPs with flexible and rigid segments generate spontaneous microphase separation due to the thermodynamic difference. As summarized in Table 1, PS-*b*-PBs and PVPDMS-*b*-PBs showed the microphase separated characteristics of two glass transition temperature (T_g) values, i.e., T_{g1}= -94~-86 °C

Table 2. Molecular compositions and thermal properties of LCBCPs and homo-mixtures.

Entry	M_n (kg/mol) [c]	PDI [c]	Phase transition (2nd heating) [g]			
			T_{g1} (°C) [d]	T_{g2} (°C) [d]	T_i (°C) [e] [ΔH_i] (J/g) [f]	ΔT (°C) [h]
PS_{3k}-*b*-(PB_{6k}-*g*-LC_2) [a]	21.3	1.05	-83	27	74 (0.2)	47
PS_{3k}-*b*-(PB_{12k}-*g*-LC_2)	37.9	1.04	-81	29	75 (0.1)	46
PS_{3k}-*b*-(PB_{18k}-*g*-LC_2)	51.8	1.04	-80	30	77 (0.1)	47
($PVPDMS_{3k}$-*g*-LC_1)-*b*-PB_{6k}	25.5	1.19	-98	29	97 (4.5)	68
($PVPDMS_{3k}$-*g*-LC_1)-*b*-PB_{18k}	35.0	1.19	-95	29	110 (5.5)	81
($PVPDMS_{3k}$-*g*-LC_1)-*b*-PB_{30k}	46.2	1.15	-94	33	112 (4.3)	79
($PVPDMS_{3k}$-*g*-LC_1)-*b*-(PB_{6k}-*g*-LC_2)	35.2	1.20	-63	15	100 (1.9)	85
($PVPDMS_{3k}$-*g*-LC_1)-*b*-(PB_{18k}-*g*-LC_2)	51.8	1.25	-65	17	***T*$_s$:57** [i] **(2.3)** [j]; T_i:114 (1.3)	97
($PVPDMS_{3k}$-*g*-LC_1)-*b*-(PB_{30k}-*g*-LC_2)	71.3	1.26	-63	22	***T*$_s$:57** [i] **(2.7)** [j]; T_i:124 (1.3)	102
($PVPDMS_{3k}$-*g*-LC_1):(PB_{6k}-*g*-LC_2)/1:1 [b]	--	--	-86	40	70 (5.2) 99(2.1)	--
($PVPDMS_{3k}$-*g*-LC_1):(PB_{6k}-*g*-LC_2)/1:2	--	--	-82	29	70(7.0) 97(0.9) 125(0.1)	--
($PVPDMS_{3k}$-*g*-LC_1):(PB_{6k}-*g*-LC_2)/1:3	--	--	-82	26	71(6.6) 96(0.1) 125(0.2)	--

[a] Mono/bi-functionalized LCBCPs with well-designed molecular weight in different blocks. [b] Mixed homopolymers of PVPDMS attached by LC_1 (PVPDMS-*g*-LC_1) and PB attached by LC_2 (PB-*g*-LC_2) in different mole ratios. [c] Number-average molecular weight (M_n) and polydispersity index (PDI), determined by GPC, [d] The first glass transition temperature (T_{g1}) and the second glass transition temperatures (T_{g2}) on the second heating cycle, [e] LC-isotropic phase transition temperature (T_i) and [f] the corresponding thermal transition absorption enthalpy (ΔH_i), [g] all determined by DSC, [h] mesomorphic temperature range ($\Delta T = T_i - T_{g2}$), [i] the smectic phase transition temperature (T_s) and [j] the corresponding thermal transition absorption enthalpy (ΔH_s).

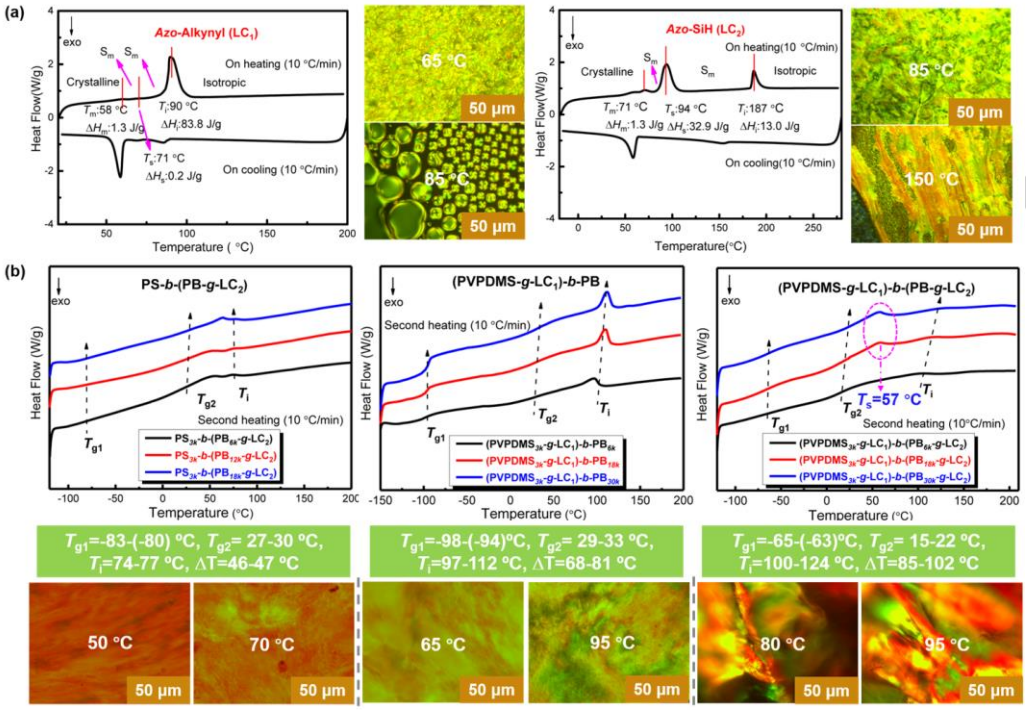

Figure 2. (a) DSC traces on heating and cooling cycles and representative POM (50 μm) images within mesogenic temperature range of *Azo*-alkynyl (LC_1) and *Azo*-SiH (LC_2) (S_m: Smectic phase; T_m: melting temperature; T_s: mesogenic phase transition temperature; T_i: LC-isotropic temperature; ΔH: the corresponding thermal transition absorption enthalpy); (b) DSC traces on the second heating cycle and the representative POM (50 μm) images within mesogenic temperature range of LCBCPs.

and T_{g2}=17~32 °C, which could be attributed to the flexible PB blocks and rigid PS/PVPDMS blocks. As shown in Figure S9, PB blocks showed a noticeable change in the slope of the DSC curves related with their T_{g1}. However, for PS-*b*-(PB-*g*-LC_2) and (PVPDMS-*g*-LC_1)-*b*-(PB-*g*-LC_2) with LC functionalization in PB blocks, PB blocks exhibited a gradual change in the slope of the DSC curves related with their T_{g1}, and T_{g1} values increased relative to those of (PVPDMS-*g*-LC_1)-*b*-PB with no functionalization in PB blocks, which are summarized in Table 2 and shown in Figure 2b. T_{g1} values were recorded in the order of (PVPDMS-*g*-LC_1)-*b*-PB (-98~-94 °C) < PS-*b*-(PB-*g*-LC_2) (-83~-80 °C) < (PVPDMS-*g*-LC_1)-*b*-(PB-*g*-LC_2) (-65~-63 °C). With regard to PS-*b*-(PB-*g*-LC_2) with no LC functionalization in PS blocks, T_{g2} values (T_{g2}=27~30 °C) were higher than those of PS blocks in PS-*b*-PBs (T_{g2}=17~21 °C). As the strong π-π stacking as an internal driving force induced LC ordering,[13] T_{g2} values were probably attributed to the π-π stacking of *Azo* mesogens aggregation. The above discussion strongly suggested the microphase separation of LCBCPs which is different from the original BCPs. We will discuss the microphase separation in terms of microstructural diameters identified by powder SAXS in the following section.

As shown in Figure 2b and Table 2, all the LCBCPs displayed two obvious T_g and one T_i values, interestingly, an exception was observed that (PVPDMS-*g*-LC_1)-*b*-(PB-*g*-LC_2) exhibited an additional T_s=57 °C when PB chain length increased. To confirm the appearance of T_s and attributions of T_g mentioned above, $PVPDMS_{3k}$-*g*-LC_1 and PB_{6k}-*g*-LC_2 were synthesized (sample preparations are shown in Supporting Information) and mixed in comparable mole ratios (1:1; 1:2; 1:3) with LCBCPs. As shown in Figure S10 and Table 2, T_{g1} (-86~-82 °C) of the mixtures were adjacent to those (-83~-80 °C) of PS-*b*-(PB-*g*-LC_2), which explained that T_{g1} of LCBCPs should be attributed to PB blocks. Moreover, the mixtures displayed different T_i values, for example, T_i (70~71 °C) of mixtures were adjacent to those (74~77 °C) of PS-*b*-(PB-*g*-LC_2) and T_i (125 °C) of mixtures appeared when the mole fractions of PB_{6k}-*g*-LC_2 in mixtures increased; T_i (96~99 °C) of mixtures were adjacent to those (97~112 °C) of (PVPDMS-*g*-LC_1)-*b*-PB. Therefore, the additional T_s=57 °C of (PVPDMS-*g*-LC_1)-*b*-(PB-*g*-LC_2) when the PB length increased (Figure 2b and Table 2) could be attributed to the mesophase of PB LC blocks.

These results discussed above of the appearance of T_s and attributions of T_g demonstrated that PB LC blocks and PVPDMS LC blocks probably maintained the independence of phase transitions in bi-functionalized (PVPDMS-*g*-LC_1)-*b*-(PB-*g*-LC_2). In addition, the competitive interactions between PVPDMS LC blocks and PB LC blocks occurred, where the influence of PB LC blocks on the phase transitions enlarged when the PB chain length increased.

The temperature range of mesogenic formation ($\Delta T=T_i-T_{g2}$) is known as an important parameter of properties. In present work, $\Delta T=T_i-T_{g2}$ was taken for further discussions. As shown in Figure 2b and Table 2, (PVPDMS-*g*-LC_1)-*b*-(PB-*g*-LC_2) (ΔT=85~102 °C) presented slightly wider ΔT values compared with (PVPDMS-*g*-LC_1)-*b*-PB (ΔT=68~81 °C), but generated dramatically wider ΔT values compared with PS-*b*-(PB-*g*-LC_2) (ΔT=46~47 °C). In addition, although *Azo*-SiH (LC_2) (ΔT=116 °C) showed a much wider ΔT value compared with *Azo*-Alkynyl (LC_1) (ΔT=32 °C), (PVPDMS-*g*-LC_1)-*b*-PB (ΔT=68~81 °C) with *Azo*-Alkynyl (LC_1) functionalization in PVPDMS blocks showed wider ΔT values than did PS-*b*-(PB-*g*-LC_2) (ΔT=46~47 °C) with *Azo*-SiH (LC_2) functionalization in PB blocks. The general tendency was demonstrated in the order of PS-*b*-(PB-*g*-LC_2) (ΔT=46~47 °C) < (PVPDMS-*g*-LC_1)-*b*-PB (ΔT=68~81 °C) < (PVPDMS-*g*-LC_1)-*b*-(PB-*g*-LC_2) (ΔT=85~102 °C) in analogies.

There are three reasons for the above phenomenon as follows. Firstly, PVPDMS LC blocks with a complete grafting could probably contribute to a stronger molecular interaction in LCBCPs compared with PB LC blocks with a low grafting density. Secondly, the flexibility and low grafting density of PB LC blocks largely disturbed the formation of LC phase, as PVPDMS-*b*-PBs and PS-*b*-PBs were designed with rigid PVPDMS/PS blocks in the minority of molecular weight (M_n=3 kg/mol) and flexible PB blocks in the majority (M_n=6~30 kg/mol) to manipulate the motions of matrixes. Thirdly, alkynyl terminals of *Azo*-Alkynyl (LC_1) had a stronger polar effect on the stability of LC phase than Si-H terminals of *Azo*-SiH (LC_2), which explained that *Azo*-SiH (LC_2) showed a much wider ΔT and a higher T_i than did *Azo*-Alkynyl (LC_1). However, the polarity decreased when alkynyl terminals of *Azo*-Alkynyl (LC_1) reacted with PVPDMS. Thus, the flexibility of both Si-O-Si spcers and PB LC blocks probably cooperatively contributed to the narrow ΔT values.

These results demonstrated that PB LC blocks and PVPDMS LC blocks had a cooperative contribution to bi-functionalized (PVPDMS-*g*-LC_1)-*b*-(PB-*g*-LC_2) in terms of the temperature range of mesogenic formation (ΔT).

X-ray analysis. The independent and cooperative effect of PB LC blocks and PVPDMS LC blocks is evident from DSC and POM results. In order to further confirm this effect and the precise arrangement of LC phase, powder WAXD and SAXS were cooperatively performed within the temperature range of mesomorphic formation. At first, it should be noted that the polymer backbone of side-chain liquid crystalline polymers (SCLCPs) tends to keep the Gaussian chain conformation while the mesogenic side groups tend to align parallel to one another to form the molecular interaction of LC phase. Hence, although the lengths of side groups should be variable depending on their conformations, we only need to measure the longest theoretical coplanar molecular length (*L*), because these values are generally smaller than the layer spacing values when taking Gaussian chain conformation into consideration, which is basic and convincing enough to confirm the arrangement of LC phase of SCLCPs. In previous work, the side groups were measured while spacers were not taken into consideration.[14] In this work, we measured the lengths of repeated units of polymers instead of side groups,[8a, 11a, 11b] which meant that the spacers were taken into consideration. As shown in Figure S11, not only *Azo*-Alkynyl (LC_1) and *Azo*-SiH (LC_2) but also repeated units of LCBCPs were simulated to obtain the longest theoretical coplanar molecular length (*L*) upon energy minimization.

WAXD. As shown in Figure S12a, *Azo*-Alkynyl (LC_1) (*L* =25.6 Å) showed two weak first-order and second-order diffractions at 2θ=2.70° (layer domain spacing: *d*=32.7 Å, calculated from the Bragg diffraction equation: 2*d*sinθ=*λ*, *λ*=1.54 Å) and 5.40° with a ratio of 1:2 in 1D WAXD (65 °C), meanwhile, the bright halo appeared near the equator and center in 2D WAXD as shown in Figure S12b. *Azo*-SiH (LC_2) (*L*=20.3 Å) showed a first-order sharp peak shift depending on temperature, i.e., 2θ=2.00° (*d*=44.1 Å ≈ 2*L*, 80 °C) and 2θ=2.18° (*d*=40.5 Å ≈ 2*L*, 120 °C), as well as the two peaks (80 °C) and a diffuse diffraction (120 °C) at wide angles. The results indicated a smectic phase of *Azo*-Alkynyl (LC_1) with an interpenetrative molecular bilayer packing (2*L* > *d*=32.7 Å > *L*) and a phase transition of smectic phase between 65 °C and 80 °C in combination with POM and DSC results. Similarly, the above results indicated a smectic phase transition and a possible bilayer arrangement of *Azo*-SiH (LC_2).

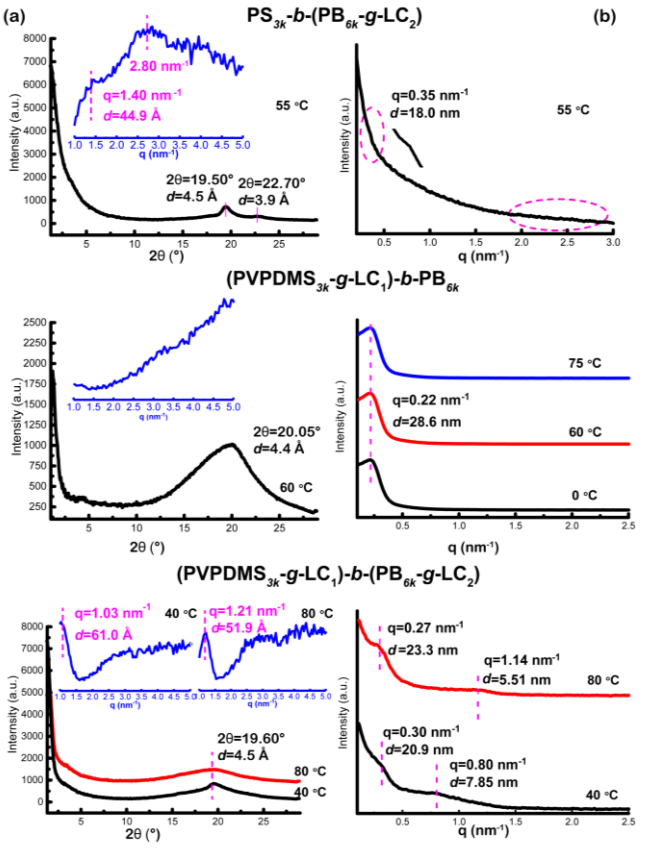

Figure 3. (a) Temperature-dependent 1D powder WAXD curves with Lorentz correction traces inside and (b) SAXS traces of LCBCPs. (Lorentz correction equation: X-axis= q= [4π sinθ]/*λ*, *λ*=1.54 Å; Y-axis= I*q^2, I=Intensity)

As for LCBCPs, there were no signals observed within 2θ<5° in 1D WAXD (Figure 3a), because the highly flexible PB blocks decreased side interactions and further disturbed the microstructural order. And then, Lorentz corrections in terms of X-axis (q=4πsinθ/*λ*, *λ*=1.54 Å) and Y-axis (I*q^2, I=Intensity) were applied, and the correction curves were observed inside the Figure 3a. After Lorentz correction of PS-*b*-(PB-*g*-LC_2) (*L*=19.7 Å), two signals at q=1.40 nm^{-1} and q=2.80 nm^{-1} (55 °C) were observed, suggesting a smectic phase with a bilayer arrangement (*d*=44.9 Å ≈ 2*L*). However, there were no obvious diffractions within 2θ<5° of (PVPDMS-*g*-LC_1)-*b*-PB, which could be attributed to the flexibility of unfunctionalized PB blocks. As shown in Figure 3a and Figure S12c, a wide diffraction (60 °C) within 5°<2θ<30° in 1D WAXD and a halo near the equator in 2D WAXD indicated the nematic phase of (PVPDMS-*g*-LC_1)-*b*-PB. In addition, (PVPDMS-*g*-LC_1)-*b*-(PB-*g*-LC_2) (*L*=28.9 Å) showed a sharp peak shift depending on temperature, i.e., q=1.03 nm^{-1} (*d*=61.0 Å ≈ 2*L*, 40 °C) and q=1.21 nm^{-1} (2*L*>*d*=51.9 Å>*L*, 80 °C), suggesting a possible bilayer molecular packing and an interpenetrative arrangement of smectic phase, and further a phase transition of smectic phase. In particular, it should be noted that (PVPDMS-*g*-LC_1)-*b*-(PB-*g*-LC_2) showed a phase transition of LC phase (T_s=57 °C) between 40 °C and 80 °C in above mentioned DSC results, which determined the appearance of PB LC blocks. In this section, we can see that (PVPDMS-*g*-LC_1)-*b*-(PB-*g*-LC_2) showed a peak shift over temperature, which further confirmed DSC results. And it was clear that PB LC blocks and PVPDMS LC blocks maintained the independence into bi-functionalized (PVPDMS-*g*-LC_1)-*b*-(PB-*g*-LC_2).

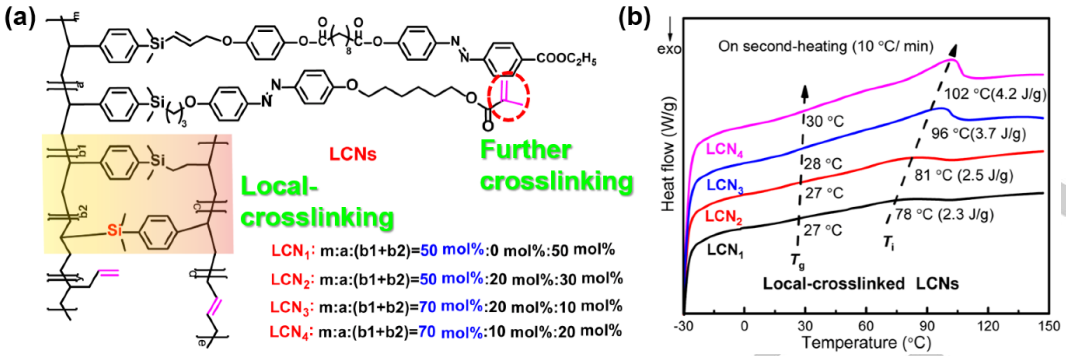

Figure 4. (a) Chemical structures of local-crosslinked LCNs with different compositions and (b) DSC curves on the second heating cycle of LCNs.

SAXS. Due to the limitation of the WAXD instrument, SAXS was further performed to assess microscopical orientation in small angle regions in combination with WAXD. As shown in Figure 3b, no signals of LC phase were detected in SAXS of (PVPDMS-*g*-LC_1)-*b*-PB, indicating a nematic phase. While a signal at q=0.22 nm^{-1} remained consistent at different temperatures, which should be ascribed to phase separated microdomain spacings (d=28.6 nm, $d=2\pi/q$) because of the rigid and flexible segments involved in diblock copolymer. In addition, PS-*b*-(PB-*g*-LC_2) showed a weak signal at q=2.5 nm^{-1} (d=25.1 Å, 55 °C). Because the flexibility and low grafting density of PB LC blocks largely disturbed the formation of LC phase, which led to a weak interaction of smectic phase. (PVPDMS-*g*-LC_1)-*b*-(PB-*g*-LC_2) showed an obvious peak shift depending on temperature, i.e., q=0.8 nm^{-1} (d=78.5 Å, 40 °C) and q=1.14 nm^{-1} (d=55.1 Å, 80 °C), which was in good accordance with the peak shift from q=1.03 nm^{-1} (d=61.0 Å, 40 °C) to q=1.21 nm^{-1}(d=51.9 Å, 80 °C) in 1D WAXD (Figure 3a). The results also provided a critical evidence for a phase transition T_s=57 °C between 40 °C and 80 °C. It was found that the layer domain spacing of (PVPDMS-*g*-LC_1)-*b*-(PB-*g*-LC_2) was much longer than that of PS-*b*-(PB-*g*-LC_2), further indicating that PVPDMS LC blocks and PB LC blocks not only maintained the independence but also had a cooperative effect on bi-functionalized (PVPDMS-*g*-LC_1)-*b*-(PB-*g*-LC_2).

Microphase separation. Generally, BCPs with characteristic rigid-flexible components tend to promote spontaneous microphase separation due to the thermodynamic differences[15]. As discussed above, PS-*b*-PBs and PVPDMS-*b*-PBs showed the characteristics of phase separation in terms of physical principles, i.e., T_{g1}= -94~-86 °C and T_{g2}=17~32 °C, which could be attributed to flexible PB and rigid PS/PVPDMS, respectively. In present work, the effect of different modular funtions on microphase separation was discussed, as the cooperative and competitive motion between different modular blocks would change the thermodynamic balance. As summarized in Table 2, DSC results displayed two T_g signals, indicating a spontaneous microphase separation. According to the above discussions, we have made a description on the attributions of different T_g values of LCBCPs. Herein, SAXS profiles were conducted to provide convincing evidence for microphase separated microdomain diameters of LCBCPs.

As mentioned above, except some signals of LC order were observed in SAXS profiles of LCBCPs, some additional signals of microphase separated order were obviously observed. For example, two weak signals at q=2.5 nm^{-1} (layer domain spacing of smectic phase: d=25.1 Å, 55 °C) and q=0.35 nm^{-1} (microphase separated microdomain diameter: d=18.0 nm) of PS-*b*-(PB-*g*-LC_2) were observed in Figure 3b. The former represented the order of smectic phase, while the latter should be attributed to the microphase separated order. With the decrease of the thermodynamic difference between PS in the minority of molecular weight (M_n=3 kg/mol) and PB blocks containing rigid LC side groups, a weak signal from microphase separated order in SAXS of PS-*b*-(PB-*g*-LC_2) was identified. (PVPDMS-*g*-LC_1)-*b*-PB showed a strong and constant signal at q=0.22 nm^{-1} over temperature because of the enlargement of thermodynamic difference between rigid PS blocks containing rigid LCs and flexible PB blocks. The microscopically orientated q=0.22 nm^{-1} indicated a disordered bicontinuous phase with phase separated microdomain diameter d=28.6 nm.[16] For (PVPDMS-*g*-LC_1)-*b*-(PB-*g*-LC_2), there was one peak shift from q=0.30 nm^{-1} (d=20.9 nm, 40 °C) to q=0.27 nm^{-1} (d=23.3 nm, 80 °C) over temperature. The changes in the microdomains of microphase separation might be attributed to the smectic phase transition (T_s=57 °C) of (PVPDMS-*g*-LC_1)-*b*-(PB-*g*-LC_2), which was best defined for the results of WAXD and DSC. Furthermore, the microphase separated microdomain diameters showed the order of PS-*b*-(PB-*g*-LC_2) <(PVPDMS-*g*-LC_1)-*b*-(PB-*g*-LC_2)<(PVPDMS-*g*-LC_1)-*b*-PB. These results suggested that PVPDMS LC blocks of (PVPDMS-*g*-LC_1)-*b*-PB and PB LC blocks of PS-*b*-(PB-*g*-LC_2) did have a cooperative contribution to (PVPDMS-*g*-LC_1)-*b*-(PB-*g*-LC_2).

Application of modular design in local-crosslinked LCNs. In the above discussion, LCBCPs with modular functionalization have been synthesized and well characterized. We are inspired to obtain local-crosslinked LCNs with reasonably designed functionality in different blocks, which will contribute to designing materials from basic molecular control, as researchers have devoted much effort to the innovation and application of LCNs in multiple functional materials.[17]

As shown in Figure 4, local-crosslinked LCNs were designed by performing a quantitative hydrosilylation of $PVPDMS_{3k}$-*b*-PB_{18k} and *Azo*-Alkynyl (LC_1) with control over temperature. At first, (PVPDMS-*g*-LC_1)-*b*-PB with rationally designed 50 mol% and 70 mol% grafting density in PVPDMS blocks were obtained at 30 °C. Afterwards, an asymmetric cross-linker (ACA) containing a pair of asymmetric double bonds, where the acrylic group was designed for a further photo-crosslinking and had no reactivities with Si-H groups, was introduced to PVPDMS blocks at 50 °C. Meanwhile, local-crosslinked LCNs with rationally designed 50 mol% and 70 mol% grafting density of (PVPDMS-*g*-LC_1)-*b*-PB were obtained through the local-crosslinked treatment of (PVPDMS-*g*-LC_1)-*b*-PB between remaining Si-H of PVPDMS blocks and double bonds of PB blocks at 50 °C.

To confirm the above modular functionalization, this process was tracked by FT-IR and ^{1}H NMR. As indicated in Figure S13a, the disappearance in FT-IR of peak at 2116 nm^{-1} assigned to Si-H groups indicated a complete addition in PVPDMS blocks. By comparison in ^{1}H NMR, the double bonds in PB blocks were consumed, but PB LC blocks showed a low grafting density served as a local-crosslinking point for good processability. According to the design in Figure 4, PVPDMS blocks had an almost 100% grafting density, where (PVPDMS-*g*-LC$_1$)-*b*-PB had 50%/70% moles of *Azo*-Alkynyl (LC$_1$), low density of ACA as photo-croslinkers, and low local-crosslinking density.

The properties of local-crosslinked LCNs were further idetified by POM and DSC analysis. As seen in POM observations in Figure S13b, LCNs presented the morphological textures of LCs upon heating and cooling. More importantly, LCNs with well-designed compositions showed room temperature T_g (T_g=27~30 °C) and well-controlled T_i values (T_i=78~102 °C) for easily processable conditions (Figure 4b). These results confirmed the design of local-crosslinked LCNs by applying the principle of building "blocks" and modular functionalization. This design provides a new principle for designing local-crosslinked LCNs, which is of both fundamental interest and potential implications.

Conclusion

In summary, LCBCPs with modular functionalization have been designed by the principle of building "blocks", where *Azo*-Alkynyl (LC$_1$) and *Azo*-SiH (LC$_2$) were independently and site-selectively incorporated into PVPDMS-*b*-PBs and PS-*b*-PBs in combination with LAP and hydrosilylation. The cooperative and independent influence of modular functionalization on mesophase and microphase separation was demonstrated. At first, PB LC blocks and PVPDMS LC blocks had cooperative contributions to the mesogenic properties and microphase separation of (PVPDMS-*g*-LC$_1$)-*b*-(PB-*g*-LC$_2$), where polarized optical morphologies showed a brighter order as PS-*b*-(PB-*g*-LC$_2$) < (PVPDMS-*g*-LC$_1$)-*b*-PB< (PVPDMS-*g*-LC$_1$)-*b*-(PB-*g*-LC$_2$), thermal properties were recorded as PS-*b*-(PB-*g*-LC$_2$) (ΔT=46~47°C) < (PVPDMS-*g*-LC$_1$)-*b*-PB (ΔT=68~81 °C) < (PVPDMS-*g*-LC$_1$)-*b*-(PB-*g*-LC$_2$) (ΔT=85~102 °C), and the microphase separated microdomain diameters showed an order as PS-*b*-(PB-*g*-LC$_2$) <(PVPDMS-*g*-LC$_1$)-*b*-(PB-*g*-LC$_2$)<(PVPDMS-*g*-LC$_1$)-*b*-PB. Secondly, PB LC blocks and PVPDMS LC blocks showed their independence in (PVPDMS-*g*-LC$_1$)-*b*-(PB-*g*-LC$_2$) because of an additional T_s=57 °C observed in (PVPDMS-*g*-LC$_1$)-*b*-(PB-*g*-LC$_2$) determined using powder X-rays analysis of LCBCPs and charactering the mixtures of PVPDMS$_{3k}$-*g*-LC$_1$ and PB$_{6k}$-*g*-LC$_2$. Thirdly, DSC results and SAXS profiles provided convincing microstructural evidence for the phase separation of LCBCPs. More importantly, by applying the principle of building "blocks" and modular functionalization, local-crosslinked LCNs were obtained and showed room temperature T_g and well-controlled T_i values (T_i=78~102 °C) for easily processable conditions by controlling molecular compositions.

Experimental Section

The materials used in the experiment and the characterizations are shown in Supporting Information. In addition, synthetic routes and related characterization results including ^{1}H NMR, FT-IR, DSC, X-ray, POM and GPC as well as experimental details and related characterization results are also shown in Supporting information.

Acknowledgements

Thankful for the financial support of the National Natural Science Foundation of China (No. 21805025, No. 21674017) and National Key R&D Program of China (2017YFB0307101) and Fundamental Research Funds for the Central Universities DUT19RC (4)001.

Keywords: Living Anionic Polymerization • Liquid Crystal Block Copolymers • Building "Blocks" • Modular Functionalization • Hydrosilylation

[1] a) E. Elacqua, A. Croom, K. B. Manning, S. K. Pomarico, D. Lye, L. Young, M. Weck, *Angew. Chem. Int. Ed.* **2016**, *55*, 15873-15878; b) Y. Wang, H. Xu, X. Zhang, *Adv. Mater.* **2009**, *21*, 2849-2864.

[2] a) P. Deshmukh, M. Gopinadhan, Y. Choo, S. K. Ahn, P. W. Majewski, S. Y. Yoon, O. Bakajin, M. Elimelech, C. O. Osuji, R. M. Kasi, *ACS Macro Lett.* **2014**, *3*, 462-466; b) F. Liao, L. Y. Shi, L. C. Cheng, S. Lee, R. Ran, K. G. Yager, C. A. Ross, *Nanoscale* **2019**, *11*, 285-293; c) M. Komura, A. Yoshitake, H. Komiyama, T. Iyoda, *Macromolecules* **2015**, *48*, 672-678; d) H. L. Xu, J. Bijleveld, M. Hedge, T. Dingemans, *Polym. Chem.* **2019**, *10*, 5052-5069; e) M. Petr, B. A. Katzman, W. DiNatale, P. T. Hammond, *Macromolecules* **2013**, *46*, 2823-2832; f) S. Nagano, Y. Koizuka, T. Murase, M. Sano, Y. Shinohara, Y. Amemiya, T. Seki, *Angew. Chem. Int. Ed.* **2012**, *51*, 5884-5888.

[3] a) H. F. Yu, *Prog. Polym. Sci.* **2014**, *39*, 781-815; b) H. B. Pan, W. Zhang, A. Q. Xiao, X. L. Lyu, P. P. Hou, Z. H. Shen, X. H. Fan, *Polym. Chem.* **2019**, *10*, 991-999; c) L. Y. Shi, F. Liao, L. C. Cheng, S. H. Lee, R. Ran, Z. H. Shen, C. A. Ross, *ACS Macro Lett.* **2019**, *8*, 852-858; d) K. Yuan, L. Chen, Y. W. Chen, *J. Mater. Chem. C* **2014**, *2*, 3835-3845; e) T. J. Wang, X. Li, Z. J. Dong, S. Huang, H. F. Yu, *ACS Appl. Mater. Interfaces* **2017**, *9*, 24864-24872.

[4] a) F. Zhou, K. H. Gu, Z. Y. Zhang, M. Y. Zhang, S. Zhou, Z. H. Shen, X. H. Fan, *Angew. Chem. Int. Ed.* **2016**, *55*, 15007-15011; b) Z. Z. Tong, Y. M. Li, H. A. Xu, H. Chen, W. J. Yu, W. Q. Zhuo, R. K. Zhang, G. H. Jiang, *ACS Macro Lett.* **2016**, *5*, 867-872.

[5] a) I. E. Serhatli, T. Kacar, *J. Appl. Polym. Sci.* **2006**, *99*, 3187-3194; b) F. Yilmaz, F. Kasapoglu, Y. Hepuzer, Y. Yagci, L. Toppare, E. G. Fernandes, G. Galli, *Des. Monomers Polym.* **2005**, *8*, 223-236; c) G. P. Mao, J. G. Wang, S. R. Clingman, C. K. Ober, J. T. Chen, E. L. Thomas, *Macromolecules* **1997**, *30*, 2556-2567; d) J. Sanger, W. Gronski, *Macromol. Chem. Phys.* **1998**, *199*, 555-561.

[6] a) N. I. Boiko, M. A. Bugakov, E. V. Chernikova, A. A. Piryazev, Y. I. Odarchenko, D. A. Ivanov, V. P. Shibaev, *Polym. Chem.* **2015**, *6*, 6358-6371; b) A. Zenati, S. Thammalangsy, *J. Polym. Sci., Part A: Polym. Chem.* **2018**, *56*, 1617-1629; c) J. Q. Jin, M. J. Tang, Z. H. Zhang, K. Zhou, Y. Gao, Z. G. Zheng, W. A. Zhang, *Polym. Chem.* **2018**, *9*, 2101-2108; d) B. Mu, X. Li, K. Y. Chen, Y. M. Zeng, J. L. Fang, D. Z. Chen, *J. Polym. Sci., Part A: Polym. Chem.* **2017**, *55*, 2544-2553.

[7] a) Y. Choo, L. H. Mahajan, M. Gopinadhan, D. Ndaya, P. Deshmukh, R. M. Kasi, C. O. Osuji, *Macromolecules* **2015**, *48*, 8315-8322; b) Y. Zhu, Y. Q. Zhou, Z. Chen, R. Lin, X. G. Wang, *Polymer* **2012**, *53*, 3566-3576; c) X. F. Chen, Z. H. Shen, X. H. Wan, X. H. Fan, E. Q. Chen, Y. G. Ma, Q. F. Zhou, *Chem. Soc. Rev.* **2010**, *39*, 3072-3101; d) Y. Liu, W. Wei, H. M. Xiong, *Polym. Chem.* **2015**, *6*, 583-590; e) Y. C. Xu, C. M. Dong, *J. Polym. Sci., Part A: Polym. Chem.* **2012**, *50*, 1216-1225; f) M. Huo, Z. Y. Wan, M. Zeng, Y. Wei, J. Y. Yuan, *Polym. Chem.* **2018**, *9*, 3944-3951.

[8] a) L. Han, H. W. Ma, S. Q. Zhu, P. B. Liu, H. Y. Shen, L. C. Yang, R. Tan, W. Huang, Y. Li, *Macromolecules* **2017**, *50*, 8334-8345; b) M. Yamada, T. Iguchi, A. Hirao, S. Nakahama, J. Watanabe, *Macromolecules* **1995**, *28*, 50-58; c) M. Walther, H. Faulhammer, H. Finkelmann, *Macromol. Chem. Phys.* **1998**, *199*, 223-237.

[9] a) Q. C. Ma, L. Han, H. W. Ma, P. B. Liu, H. Y. Shen, L. C. Yang, C. Li, X. Y. Hao, Y. Li, *Polymer* **2019**, *184*, 121907; b) L. C. Yang, L. Han, H. W. Ma, P. B. Liu, H. Y. Shen, C. Li, S. B. Zhang, Y. Li, *Chin. J. Polym. Sci.* **2019**, *37*, 841-850; c) W. Huang, H. W. Ma, L. Han, P. B. Liu, L. C. Yang, H. Y. Shen, X. Y. Hao, Y. Li, *Macromolecules* **2018**, *51*, 3746-3757.

[10] a) Y. Tsai, J. H. Wu, C. H. Li, Y. T. Wu, M. T. Leu, *J. Appl. Polym. Sci.* **2010**, *116*, 172-178; b) A. Hasebe, Y. Suematsu, S. Takeoka, T. Mazzocchi, L. Vannozzi, L. Ricotti, T. Fujie, *ACS Biomater. Sci. Eng.* **2019**, *5*, 5734-5743.

[11] a) L. Han, H. W. Ma, Y. Li, J. Wu, H. Y. Xu, Y. R. Wang, *Macromolecules* **2015**, *48*, 925-941; b) L. Han, H. W. Ma, Y. Li, S. Q. Zhu, L. C. Yang, R. Tan, P. B. Liu, H. Y. Shen, W. Huang, X. C. Gong, *Macromolecules* **2016**, *49*, 5350-5365; c) B. Wang, H. W. Ma, K. H. Shen, D. Jun, Y. Li, *Chin. Chem. Lett.* **2012**, *23*, 1419-1422.

[12] a) Z. C. Jiang, Y. Y. Xiao, X. Tong, Y. Zhao, *Angew. Chem. Int. Ed.* **2019**, *58*, 5332-5337; b) T. Ube, K. Kawasaki, T. Ikeda, *Adv. Mater.* **2016**, *28*, 8212-8217; c) Y. Y. Liu, W. Wu, J. Wei, Y. L. Yu, *ACS Appl. Mater. Interfaces* **2017**, *9*, 782-789.

[13] M. Anthamatten, J. S. Wu, P. T. Hammond, *Macromolecules* **2001**, *34*, 8574-8579.

[14] E. Verploegen, T. Zhang, N. Murlo, P. T. Hammond, *Soft Matter* **2008**, *4*, 1279-1287.

[15] a) S. Suarez-Suarez, G. A. Carriedo, A. P. Soto, *Chem. Eur. J.* **2016**, *22*, 4483-4491; b) W. Lee, S. Park, Y. Kim, V. Sethuraman, N. Rebello, V. Ganesan, D. Y. Ryu, *Macromolecules* **2017**, *50*, 5858-5866.

[16] a) J. M. Widin, A. K. Schmitt, A. L. Schmitt, K. Im, M. K. Mahanthappa, *J. Am. Chem. Soc.* **2012**, *134*, 3834-3844; b) I. Villaluenga, X. C. Chen, D. Devaux, D. T. Hallinan, N. P. Balsara, *Macromolecules* **2015**, *48*, 358-364; c) L. Y. Zhang, T. T. Cui, X. Cao, C. J. Zhao, Q. Chen, L. X. Wu, H. L. Li, *Angew. Chem. Int. Ed.* **2017**, *56*, 9013-9017.

[17] a) T. H. Ware, M. E. McConney, J. J. Wie, V. P. Tondiglia, T. J. White, *Science* **2015**, *347*, 982-984; b) Y. Yang, E. M. Terentjev, Y. B. Zhang, Q. M. Chen, Y. Zhao, Y. Wei, Y. Ji, *Angew. Chem. Int. Ed.* **2019**, 58, 17474-17479.

10.1002/chem.202000268

WILEY-VCH

Cooperative and Independent Effect of Modular Functionalization on Mesomorphic Performances and Microphase Separation of Well-Designed Liquid Crystalline Diblock Copolymers

Lan Lei, Dr. Li Han,* Prof. Hongwei Ma, Ruixue Zhang, Shuai Huang, Heyu Shen, Lincan Yang, Chao Li, Songbo Zhang, Hongyuan Bai, Qingchi Ma, and Prof. Yang Li*

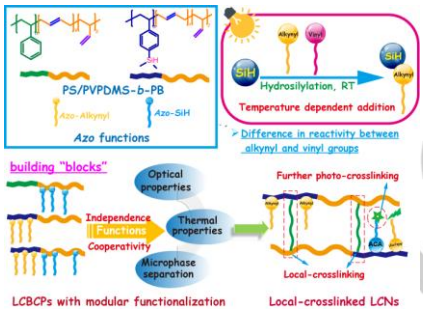

By the principle of building “blocks”, site-selective functionalized LCBCPs with modular functionalization were synthesized through LAP and temperature dependent hydrosilylation. The mono-functionalized LCBCPs showed the independence and cooperativity of different functions in bi-functionalized LCBCPs. Furthermore, LCNs with a low local-crosslinking density displayed easily processable conditions and were capable of a further photo-crosslinking.